Princeton Plasma Physics Laboratory

PPPL- 4966

PPPL- 4966

Understanding High Harmonics Ion Cyclotron Heating Losses in the Scrape-off Layer of Tokamak Plasmas

N. Bertelli, et. al.

DECEMBER, 2013

PPPL PRINCETON PLASMA PHYSICS LABORATORY

Prepared for the U.S. Department of Energy under Contract DE-AC02-09CH11466.

Princeton Plasma Physics Laboratory
Report Disclaimers

Full Legal Disclaimer

Trademark Disclaimer

PPPL Report Availability

Princeton Plasma Physics Laboratory:

http://www.pppl.gov/techreports.cfm

Office of Scientific and Technical Information (OSTI):

http://www.osti.gov/bridge

Related Links:

U.S. Department of Energy

Office of Scientific and Technical Information

Fusion Links

Understanding High Harmonics Ion Cyclotron Heating Losses in the Scrape-off Layer of Tokamak Plasmas

N. Bertelli,[1,*] E. F. Jaeger,[2] J. C. Hosea,[1] C. K. Phillips,[1] L. Berry,[3] S. P. Gerhardt,[1] D. Green,[3] B. LeBlanc,[1] R. J. Perkins,[1] P. M. Ryan,[3] G. Taylor,[1] E. J. Valeo,[1] and J. R. Wilson[1]

[1] *Princeton Plasma Physics Laboratory, Princeton, New Jersey 08543, USA*
[2] *XCEL Engineering Inc., 1066 Commerce Park Drive, Oak Ridge, Tennessee 37830, USA*
[3] *Oak Ridge National Laboratory, Post Office Box 2008, Oak Ridge, Tennessee 37831-6169, USA*

(Dated: November 14, 2013)

Full wave simulations of fusion plasmas show a direct correlation between the location of the fast-wave cut-off, radiofrequency (RF) field amplitude in the scrape-off layer (SOL) and the RF power losses in the SOL observed in the National Spherical Torus eXperiment (NSTX). In particular, the RF power losses in the SOL increase significantly when the launched waves transition from evanescent to propagating in that region. Subsequently, a large amplitude electric field occurs in the SOL, driving RF power losses when a proxy collisional loss term is added. A 3D reconstruction of absorbed power in the SOL is presented showing agreement with the RF experiments in NSTX. Loss predictions for the future experiment NSTX-Upgrade (NSTX-U) are also obtained and discussed.

In fusion experiments, external heating power using fast waves at harmonics of the ion cyclotron range of frequency (ICRF) [1] is crucial to sustain and control the plasma performance and will play an important role in the International Thermonuclear Experimental Reactor (ITER) experiment. Experimental studies of high harmonic fast wave (HHFW) heating on the National Spherical Torus eXperiment (NSTX) [2] have demonstrated that substantial HHFW power loss (up to 60% of the coupled HHFW power can be lost) can occur along the open field lines in the scrape-off layer (SOL) when edge densities are high enough that the fast waves can propagate close to the launcher, but the mechanism behind the loss is not yet understood [3–7]. Full wave simulations of selected NSTX discharges with the extended full wave code AORSA [8], in which the edge plasma beyond the last closed flux surface (LCFS) is included in the solution domain, have found standing modes in the scrape-off region for specific wavenumbers launched by the antenna [9], but the kinetic damping terms contained in the full hot plasma dielectric response are insignificant in the cold, lower density plasmas in the SOL. In this Letter we go a step further in understanding the HHFW power losses with full wave simulations, demonstrating for the first time a direct correlation between the location of the fast wave cut-off layer, the large amplitude of the RF fields in the scrape-off region, and the power losses in the SOL (driven by the RF field) observed in the NSTX experiments. In particular, a strong transition to higher SOL power losses has been found when the FW cut-off is removed from in front of the antenna with increasing edge density, consistent with the experimental observations [4]. In other words, when evanescent waves become propagating waves in the SOL, due to higher density in front of the antenna, the power losses start to increase significantly, commensurate with the amplitude of the RF field found in the SOL. The full 3D reconstruction shows that the absorbed power in the SOL is largest near the LCFS and near the front of the antenna, as experimentally observed. Finally, for the first time, full wave simulations have been used to predict that plasmas in NSTX-Upgrade (NSTX-U) will have a wider operating SOL density range in which RF power losses in the SOL are low.

In these numerical studies we make use of the full wave code AORSA that solves the Helmholtz wave equation for a tokamak geometry, including the SOL region beyond the LCFS where the magnetic field lines are open [8, 9]. AORSA includes the complete non-local, integral operator for the dielectric tensor that is valid for "all orders", namely, AORSA takes into account all contributions in $k_\perp \rho_\mathrm{i}$ ($k_\perp$, ρ_i are the perpendicular component of the wave vector relative to the local equilibrium magnetic field and the ion Larmor radius, respectively). This is essential for NSTX HHFW in which the ion Larmor radius is larger than the perpendicular wavelength and the ion-cyclotron harmonic number is large. In addition, AORSA utilizes a Fourier decomposition in the Cartesian coordinates x and y (in the poloidal plane) and in the toroidal direction of symmetry (ϕ), $e^{in_\phi \phi}$ (n_ϕ is the toroidal wave number). The density profile in the SOL is described by an exponential decay from the LCFS and a minimum density in front of the antenna, n_ant. The density decay can be modified in order to fit as best as possible the experimental data [9]. In this Letter we analyze primarily the NSTX discharge 130608 discussed in several previous works [5, 9, 10].

Figure 1 shows the wave electric field amplitude obtained with the 2D full wave code AORSA for a single (dominant) toroidal mode, $n_\phi = -21$, which corresponds to an antenna phase of $-150°$ in (a) and for $n_\phi = -12$, which corresponds to an antenna phase of $-90°$, in (b). Six different cases of the density in front of the antenna (indicated in white) are plotted for both antenna phases

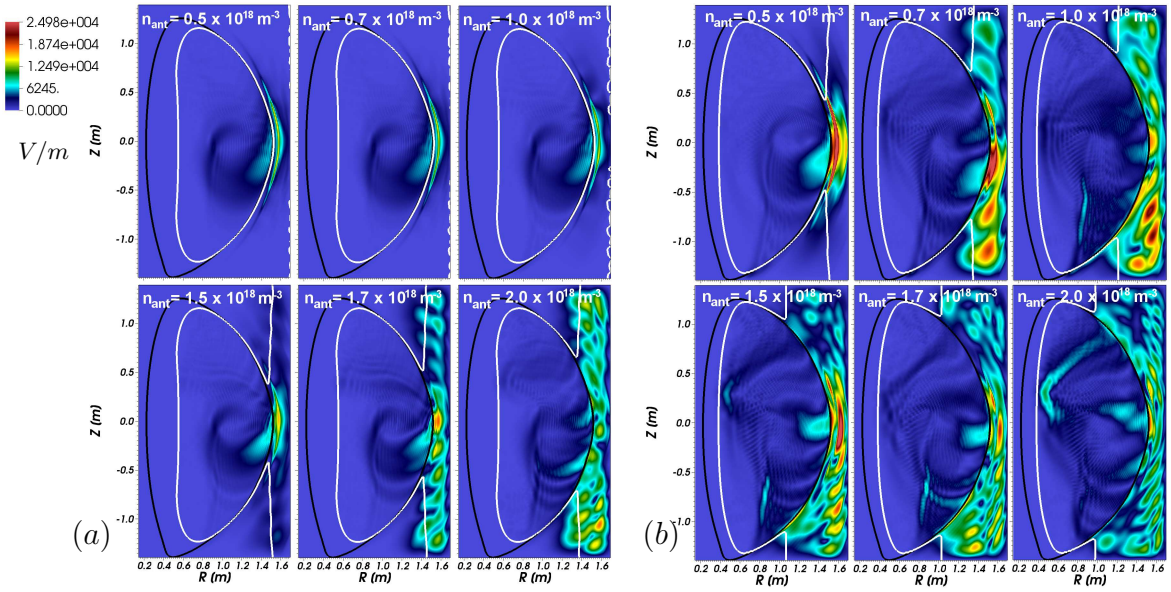

FIG. 1. Electric field amplitude for different density values in front of the antenna ($n_{\rm ant}$) (shown in the plots) with toroidal mode numbers $n_\phi = -21$ (a) and $n_\phi = -12$ (b). The white and black curves indicate the FW cut-off layer and the last closed flux surface, respectively.

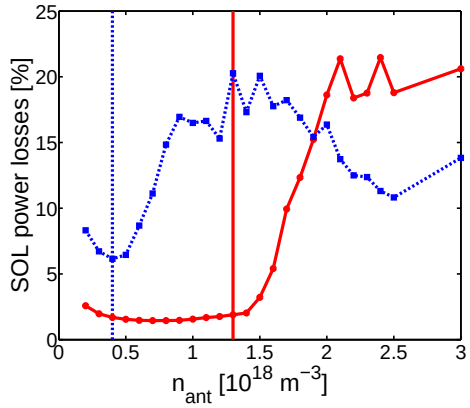

FIG. 2. Fraction of power lost to the SOL as a function of the density in front of the antenna for $n_\phi = -21$ (solid curve) and $n_\phi = -12$ (dashed curve). The vertical lines represent the value of the density for which the FW cut-off starts to be "open" in front of the antenna (see Fig. 1).

together with the contour (in white) corresponding to the FW cut-off in the cold plasma approximation. The black curves indicate the LCFS. From this figure we can clearly see that as soon as the density in front of the antenna increases sufficiently to "open" the FW cut-off in front of the antenna, the wave electric field amplitude in the SOL increases strongly. In other words, these simulations show a strong correlation between the location of the FW cut-off layer with the large electric field amplitude: when the FWs are no longer cut-off in front of the antenna and instead are propagating, the electric field amplitude outside of the LCFS increases. When the FW cut-off is "closed" in front of the antenna and the waves are evanescent, we do not predict a large RF field amplitude in the SOL. It is also important to note that for very low density we found that the RF field is strongly peaked radially and localized in front of the antenna, because the wave is strongly evanescent. For high density, when the wave is propagating, standing waves appear to form outside of LCFS independent of the launched wavenumber selected. In fact, these results appear for both antenna phases shown. Furthermore, it appears that with increasing density, the RF field amplitude in the SOL increases but not monotonically. The above effects are more evident for $n_\phi = -12$ (Figure 1(b)).

In order to understand whether the large wave electric field amplitude is one of the main drivers of the SOL power losses found in the NSTX experiments, we have inserted into AORSA an artificial "collisional" damping mechanism as a proxy to represent the actual mechanism(s) which is(are) presently unknown [11]. Specifically, a collisional frequency, ν, has been implemented as the imaginary part of the angular frequency, ω, in the argument of the Plasma Dispersion function, Z:

$$Z\left(\frac{\omega - n\omega_{\rm c}}{k_\parallel v_{\rm th}}\right) \longrightarrow Z\left(\frac{\omega - n\omega_{\rm c} + i\nu}{k_\parallel v_{\rm th}}\right), \qquad (1)$$

where n is the harmonic number, $\omega_{\rm c}$ is the cyclotron frequency, $k_\parallel$ is the parallel (to the magnetic field) component of the wave vector, and $v_{\rm th}$ is the thermal velocity. The term ν/ω is then an AORSA input parameter and allows us to adopt this specific proxy for a commensurate prediction of the power losses in the SOL region and, in particular, their behavior as a function of the density in

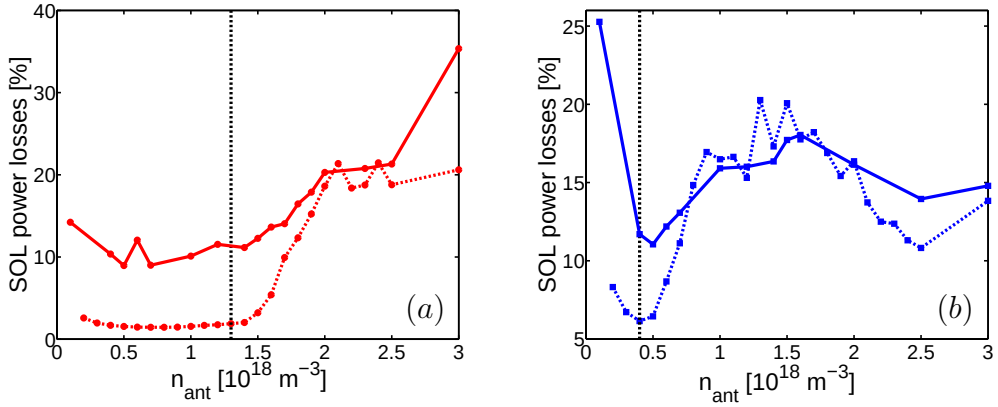

FIG. 3. Fraction of power lost to the SOL as a function of the density in front of the antenna, comparing the 3D runs (solid curves) with the dominant mode runs (dashed curves), for $n_\phi = -21$ (a) and $n_\phi = -12$ (b). The vertical lines represent the value of the density for which the FW cut-off starts to be "open" in front of the antenna.

front of the antenna. It is important to remember that without an added damping mechanism such as this proxy in the SOL, no significant SOL power losses are predicted in the simulations even in the presence of a large electric field amplitude (as shown in Figure 1). Figure 2 shows the predicted absorbed power in the SOL region (SOL power losses) as a function of the density in front of the antenna ($n_{\rm ant}$) assuming $\nu/\omega = 0.01$. Two different antenna phases are shown: $n_\phi = -12$ (dashed curve) and -21 (solid curve). Here, the cut-off of the fast wave, $n_{\rm e,FWcut-off}$, corresponds to the right hand cut-off [12]. In the HHFW frequency range, since the wave frequency is much higher than the local fundamental ion cyclotron frequency and much lower than the local lower hybrid frequency, the FW cut-off density is given by [3, 4]

$$n_{\rm e,FWcut-off} \propto \frac{k_\parallel^2 B}{\omega}, \qquad (2)$$

where B is the equilibrium magnetic field. The vertical line in Figure 2, for both cases, represents the density at which the cut-off starts to be "open" in front of the antenna, i.e., when the wave is propagating in front of the antenna and the amplitude of the electric field starts to increase in the SOL region as shown in Figure 1. Therefore, from Figure 2 one can note a rapid transition in the fraction of the power lost to the SOL from the evanescent region to the propagating region both for $n_\phi = -12$ and -21. Moreover, for lower n_ϕ ($n_\phi/R = k_\phi \sim k_\parallel$) the transition occurs at lower $n_{\rm ant}$ as expected from Eq.2. When the cut-off is "closed" in front of the antenna and therefore the wave is evanescent without a large SOL RF field amplitude, the fraction of power lost to the SOL is found to be smaller with respect to the region in which the cut-off is "open" and the wave propagating in the SOL has a large RF field amplitude. For very low density the RF power losses tend to increase again with decreasing density due to the fact that the wave is strongly evanescent such that the power can be only damped in front of the antenna, consistent with the large electric field localized in front of the antenna as indicated in Figure 1. This effect is more evident for the $n_\phi = -12$ than $n_\phi = -21$ because of the significant shift of the FW cut-off density toward lower density and, as a consequence, a narrower density range for the evanescent region. For a case with $n_\phi = -5$ corresponding to the antenna phase of $-30°$ (not shown), the transition density range is even narrower than the other two cases such that the very low density induced field dominates the electric field behavior across the evanescent region. This is due to the fact that the density value for which the FW cut-off starts to be "open" in front of the antenna is indeed very low. As a further confirmation of this result, we did the same numerical analysis (not shown) for another independent NSTX discharge, 130621, and the same edge loss transitions have been found.

A comparison of the fraction of the power lost to the SOL evaluated in the 2D poloidal cross section by AORSA (with one single dominant toroidal mode), as shown above, and in 3D using 81 toroidal modes to reconstruct the full antenna spectrum is shown in Figure 3. The solid (dashed) curves indicate the 3D (2D) results for $n_\phi = -21$ (a) and $n_\phi = -12$ (b), respectively. The 3D results exhibit similar behavior to that of the dominant mode (2D) runs and, in particular reproduce a similar transition in SOL power losses as a function of the density in front of the antenna, although it is less pronounced due to the contribution of the several toroidal modes. Larger SOL power losses in 3D runs with respect to the 2D runs are found for low and high $n_{\rm ant}$ and for both antenna phases. From the 3D AORSA runs we have obtained the 3D absorbed power deposition in the SOL, as shown in Figure 4 for $n_{\rm ant} = 2.5 \times 10^{18}$ m^{-3} and three different ρ slices (ρ is the square root of the normalized poloidal flux): $\rho = 1.1$ to 1.15, near the antenna in Fig. 4(a), $\rho = 1.05$ to 1.1 in Fig. 4(b), $\rho = 1$ to 1.05, near the LCFS in Fig. 4(c) (the antenna is at

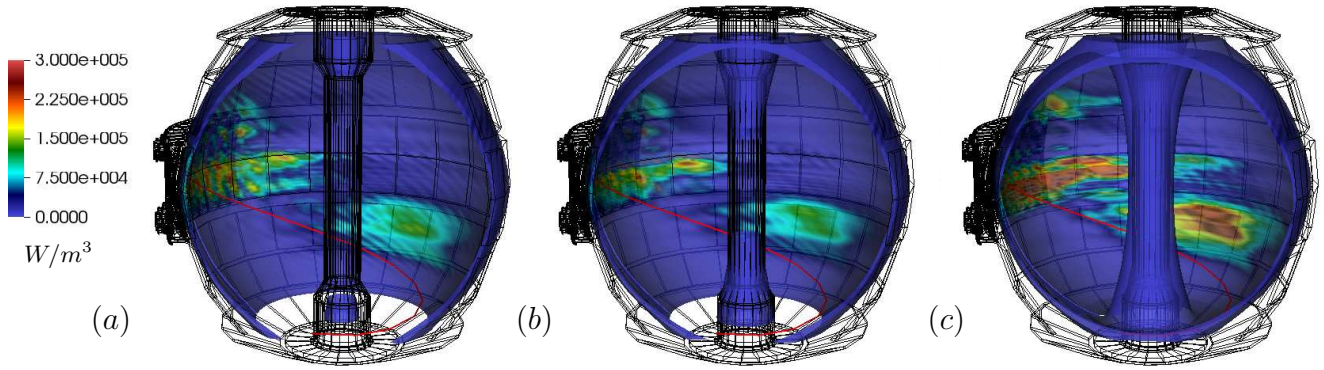

FIG. 4. 3D contour plots of the absorbed power in the SOL for three diffrent ρ slices: (a)$\rho = 1.1$ to 1.15 (near the antenna located at $\rho \simeq 1.15$), (b) $\rho = 1.05$ to 1.1, and (c) $\rho = 1$ to 1.05 (near the LCFS). The density in front of the antenna is $n_{\rm ant} = 2.5 \times 10^{18}$ m$^-3$ assuming $\nu/\omega = 0.01$. The red curve represents a magnetic field line starting from the antenna and shows the large pitch angle of the magnetic field with respect to the antenna.

$\rho \simeq 1.15$). The NSTX discharge analyzed is 130608 assuming $\nu/\omega = 0.01$. From these figures it appears that (i) the SOL power losses are larger near the antenna (cf. Fig.4(a)), and near the LCFS (cf. Fig.4(c)) consistent with the experimental studies (see Figure 11 and 12 of [7]) (the flux surface average of the absorbed power is about 1.75×10^4 W/m^3 at $\rho = 1.15$ (at the antenna location), 0.8×10^4 W/m^3 at $\rho = 1.05$, and 1.35×10^4 W/m^3 at $\rho = 1$ (at the LCFS)) ; and (ii) large SOL power losses below the mid-plane due to the large RF field.

We can now extend our numerical analysis to the NSTX-U experiment, which will be operating at the end of 2014 [13], in order to make some predictions on the behavior of the RF power losses in future NSTX-U discharges. We analyze an H-mode scenario being considered for NSTX-U with $B_{\rm T} = 1$ T, obtained by using the TRANSP code [14]. This toroidal magnetic field corresponds to the full toroidal magnetic field that will be available for the NSTX-U experiment. Figure 5 shows the predicted RF power losses in the SOL as a function of $n_{\rm ant}$ for this NSTX-U case. Exactly the same transition behavior found in the NSTX case is predicted for the NSTX-U case for both $n_\phi = -21$ (solid curve) and $n_\phi = -12$ (dashed curve). The main important difference with respect to the NSTX case is that the transition to higher losses in the SOL occurs at higher density. This is explained by the fact that the FW cut-off is proportional to the magnetic field (see Eq. 2), and therefore for the NSTX-U case with $B_{\rm T} = 1$ T the transition occurs for about a factor of two higher in density with respect to NSTX case with $B_{\rm T} = 0.55$ T (compare vertical lines in Figures 2 and 5 for each n_ϕ). This result tells us that the evanescent region for NSTX-U, in which the SOL power losses are smaller, will be wider than the one in NSTX and therefore from the experimental point of view there will be a wider SOL density range in which the experiment can run with lower SOL power losses.

The results shown in this Letter might appear to be counter-intuitive in the sense that for low density in front of the antenna the wave is evanescent and, in principle, the antenna-plasma coupling is relatively poor; and vice-versa, for high density the wave is propagating and the antenna-plasma coupling is relatively good. However, with these simulations we have demonstrated that too high density in front of the antenna, although positive for the antenna-plasma coupling, leads to substantial increases of the RF electric field in the SOL and corresponding RF power losses. As a result, from the experimental point of view, it is crucial to be able to optimize the density in SOL region in order to balance the antenna coupling and the RF power losses in the SOL. For the NSTX-U experiment, this optimization will be more easily facilitated with respect to NSTX due to the fact that, with higher magnetic field, the transition between the evanescent and the propagating region will be at a higher density $n_{\rm ant}$ since the cut-off density value is directly proportional to the magnetic field. These results suggest that SOL power losses such as predicted here, may also prove to be important for ICRF heating on ITER. Though, it is important to note that ITER will employ minority ion cyclotron heating with excitation in the range of the third harmonic of the deuterium ion cyclotron frequency, a much lower value than the $\sim 11^{\rm th}/12^{\rm th}$ harmonic excited on NSTX. Some insight into the effect of reducing the harmonic value will be obtained on NSTX-U, for which excitation will be at the $\sim 5^{\rm th}/6^{\rm th}$ harmonic. Also, the geometry and the main plasma parameters are very different on ITER with respect to the NSTX and NSTX-U experiments; e.g., the considerably smaller pitch of the magnetic field on ITER and its larger size combine to make the field line length from the lower to upper divertor strike points much greater on ITER than NSTX/NSTX-U. Therefore, in order to develop conclusive predictions for ITER, further studies, from both the experimental and theoretical point of view, are necessary in order to identify the ac-

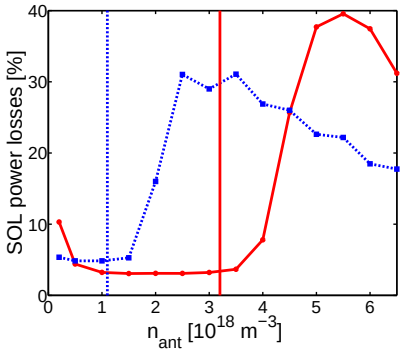

FIG. 5. Fraction of power lost to the SOL as a function of the density in front of the antenna for $n_\phi = -21$ (solid curve) and $n_\phi = -12$ (dashed curve), for an NSTX-U case with $B_\mathrm{T} = 1$ T. The vertical lines represent the value of the density for which the FW cut-off starts to be "open" in front of the antenna.

tual physical mechanism(s) behind the RF power losses in NSTX. Nevertheless, the optimization of the density in the SOL region could prove to be crucial for the performance of the ICRF heating system in ITER since the distance between wall and separatrix is large ($\sim$ 20 cm).

This work was supported by the SciDAC Center for Wave-Plasma Interactions under DE-FC02-01ER54648 and the US DOE under DE-AC02-CH0911466.

* nbertell@pppl.gov

[1] M. Ono, Phys. Plasmas **2**, 4075 (1995).
[2] M. Ono and et al, Nucl. Fusion **40**, 557 (2000).
[3] J. C. Hosea and et al, Phys. Plasmas **15**, 056104 (2008).
[4] C. K. Phillips and et al, Nucl. Fusion **49**, 075015 (2009).
[5] G. Taylor and et al, Phys. Plasmas **17**, 056114 (2010).
[6] R. J. Perkins and et al, Phys. Rev. Lett. **109**, 045001 (2012).
[7] R. J. Perkins and et al, Nucl. Fusion **53**, 083025 (2013).
[8] E. F. Jaeger and et al, Phys. Plasmas **8**, 1573 (2001).
[9] D. L. Green and et al, Phys. Rev. Lett. **107**, 145001 (2011).
[10] J. C. Hosea and et al, in *AIP Conf. Proc.*, Vol. 1187 (2009) p. 105.
[11] N. Bertelli and et al, to be published in AIP Conf. Proc. (2013).
[12] T. H. Stix, *Waves in Plasmas* (American Institute of Physics, NY, 1992).
[13] J. E. Menard and et al, Nucl. Fusion **52**, 083015 (2012).
[14] S. P. Gerhardt, R. Andre, and J. E. Menard, Nucl. Fusion **52**, 083020 (2012).

The Princeton Plasma Physics Laboratory is operated
by Princeton University under contract
with the U.S. Department of Energy.

Information Services
Princeton Plasma Physics Laboratory
P.O. Box 451
Princeton, NJ 08543

Phone: 609-243-2245
Fax: 609-243-2751
e-mail: pppl_info@pppl.gov
Internet Address: http://www.pppl.gov